0038-075C/97/1626-383-398$03.00/0
Soil Science

June 1997
Vol. 162, No. 6
Printed in U.S.A.

ESTIMATING UNSATURATED SOIL HYDRAULIC PROPERTIES FROM MULTIPLE TENSION DISC INFILTROMETER DATA

Jiří Šimůnek and Martinus Th. van Genuchten

In a previous study, we showed that the cumulative infiltration rate measured with a tension disc infiltrometer at one particular tension does not provide enough information to estimate van Genuchten's soil-hydraulic parameters by numerical inversion of the Richards equation. In this paper we analyze the possibility of using cumulative infiltration rates obtained at several consecutive tensions for the purpose of estimating soil hydraulic parameters. We also investigate whether additional, easily obtainable information improves identifiability of the unknown parameters. The study is carried out using numerically generated data. The uniqueness problem was analyzed by studying the behavior of response surfaces in the optimized parameter planes. Our parameter estimation procedure combines the Levenberg-Marquardt nonlinear parameter optimization method with a quasi three-dimensional numerical model, HYDRUS-2D, which solves the variably-saturated flow equation. We found that the combination of multiple tension cumulative infiltration data with measured values of the initial and final water contents yielded unique solutions of the inverse problem for the unknown parameters.

TENSION disc infiltrometers are being used increasingly for in-situ measurement of unsaturated soil hydraulic properties (Perroux and White 1988; Ankeny et al. 1991; Reynolds and Elrick 1991; Logsdon and Jaynes 1993, among many others). Tension infiltrometers are also useful for quantifying the effects of macropores and preferential flow paths on infiltration in the field. Thus far, tension infiltration data have been used primarily for evaluating the saturated hydraulic conductivity K_s and the sorptivity parameter α^* in Gardner's exponential model (Gardner 1958) of the unsaturated hydraulic conductivity. Compared with this approximate analytical approach, relatively little work has been done in simulating unsaturated flow underneath a disc permeameter using more complete numerical solutions of the Richards' equation (Quadri et al. 1994; Warrick 1992), and even fewer attempts have been made to estimate the unsaturated soil hydraulic properties (including the soil-water retention curve) from tension disc infiltration experiments by means of inverse solutions of the Richards' equation (Šimůnek and van Genuchten 1996).

Šimůnek and van Genuchten (1996) showed previously that infiltration data measured with a tension disc infiltrometer at constant tension does not yield enough information to estimate, by numerical inversion, more than two parameters in van Genuchten's (1980) analytical description of the soil hydraulic properties. They concluded that in order to obtain three soil-hydraulic parameters (α, n, and K_s) one must have additional information of the transient flow process, such as measured pressure heads below the infiltration disc inside the soil profile. Experimental experience (Clothier et al. 1992; Angulo Jaramillo et al. 1996; M. Flury, D. Wang, personal communication) suggests that because of local scale soil variability, transient flow fields below the tension infiltration disc can be relatively asymmetric, and, thus, it may be difficult to use tension infiltrometer data in a parameter optimization process. A major advantage of tension infiltrometers is their simplicity of use. This advantage is partly lost if additional measuring devices, such as tensiometers or TDRs, must be installed in the soil profile.

In this paper we analyze the possibility of using an infiltration curve obtained with a tension disc infiltrometer at several consecutive tensions

U.S. Salinity Laboratory, USDA, ARS, 450 West Big Springs Road, Riverside, CA 92507–4617. Dr. Šimůnek is corresponding author. E-mail: jsimunek@ussl.ars.usda.gov

Received Oct. 11,1996; accepted Jan. 8, 1997.

for the purpose of estimation soil hydraulic parameters. We also analyze whether additional easily obtainable information, such as the final water content below the tension disc permeameter or use of the Wooding's (1968) analytical solution in combination with numerical inversion of the Richards equation, improves identifiability of the unknown parameters.

THEORY

The governing flow equation for radially symmetric isothermal Darcian flow in a variably saturated isotropic rigid porous medium, assuming that the air phase plays an insignificant role in the liquid flow process, is given by the following modified form of the Richards' equation (Warrick 1992):

$$\frac{\partial \theta}{\partial t} = \frac{1}{r}\frac{\partial}{\partial r}\left[rK\frac{\partial h}{\partial r}\right] + \frac{\partial}{\partial z}\left[K\frac{\partial h}{\partial z}\right] + \frac{\partial K}{\partial z} \quad (1)$$

where θ is the volumetric water content [L^3L^{-3}], h is the pressure head [L], K is the hydraulic conductivity [LT^{-1}], r is a radial coordinate [L], z is vertical coordinate [L] positive upward, and t is time [T]. Note that in Eq (1) we do not consider root water uptake by plant roots since this process can probably be neglected at the time scale of a tension disc infiltration experiment, and that we assume that the porous medium is isotropic. Eq. (1) was solved numerically for the following initial and boundary equations applicable to a disc tension infiltrometer experiment (Warrick 1992):

$$h(r,z,t) = h_i \qquad t = 0 \quad (2)$$

$$h(r,z,t) = h_0(t) \qquad 0 < r < r_0,\ z = 0 \quad (3)$$

$$-\frac{\partial h(r,z,t)}{\partial z} - 1 = 0 \qquad r > r_0,\ z = 0 \quad (4)$$

$$h(r,z,t) = h_i \qquad r^2 + z^2 \to \infty \quad (5)$$

where h_i is the initial pressure head [L], h_0 is the time-variable supply pressure head imposed by tension disc infiltrometer [L] and r_0 is the disc radius [L]. Eq. (1), subject to the above initial and boundary conditions, was solved using a quasi three-dimensional (axisymmetric) finite element code, HYDRUS-2D, as documented by Šimůnek et al. (1996). The numerical solution was based on the mass-conservative iterative scheme proposed by Celia et al. (1990).

A model of the unsaturated soil hydraulic properties must be selected before application of the numerical solution of the Richards' equation. In this study we will limit ourselves to unsaturated soil hydraulic functions of the form (van Genuchten 1980):

$$\theta_e(h) = \frac{\theta(h) - \theta_r}{\theta_s - \theta_r} = \frac{1}{(1 + |\alpha h|^n)^m} \qquad h < 0 \quad (6)$$

$$\theta(h) = \theta_s \qquad h \geq 0$$

$$K(\theta) = K_s\theta_e^l[1 - (1 - \theta_e^{1/m})^m]^2 \qquad h < 0 \quad (7)$$

$$K(\theta) = K_s \qquad h \geq 0$$

where θ_e is the effective water content [−], K_s is the saturated hydraulic conductivity [LT^{-1}], θ_r and θ_s denote the residual and saturated water contents [L^3L^{-3}], respectively, l is the pore-connectivity parameter [−], and α [L^{-1}], n [−], and m ($= 1 - 1/n$) [−] are empirical parameters. The predictive $K(\theta)$ model is based on the capillary theory of Mualem (1976) in conjunction with Eq (7). The pore-connectivity parameter l in the hydraulic conductivity function was estimated by Mualem (1976) to be about 0.5 as an average for many soils. The hydraulic characteristics defined by Eqs (6) and (7) contain five unknown parameters: θ_r, θ_s, α, n, and K_s. The saturated hydraulic conductivity, K_s, and the saturated water content, θ_s, are viewed in this paper as fitted values of the hydraulic conductivity and the water content, respectively, at zero pressure head (Šimůnek and van Genuchten 1996). In reality, the saturated hydraulic conductivity, K_s, and the saturated water content, θ_s, might be different from this value due to the effects of macropores that may saturate only after a zero or positive pressure head has been applied (Logsdon et al. 1993). Because saturation will never be reached during tension infiltration experiment, K_s and θ_s in this study are interpreted as being extrapolated, empirical parameters outside the range of the disc experiment (Šimůnek and van Genuchten 1996). Also, tension disc infiltration in general is a wetting process (assuming that one can neglect internal drainage at the initial pressure head), which means that the hydraulic parameters in Eqs (6) and (7) should represent wetting branches of the unsaturated hydraulic properties.

In the analysis below we will concentrate on the optimization of only four parameters, that is α, n, θ_s, and K_s, assuming that the residual water content can be set equal to zero or obtained independently, for example from soil survey data.

FORMULATION OF THE INVERSE PROBLEM

The objective function Φ, which is minimized during the parameter estimation process

and which can be used to construct response surfaces, can be formulated either using only cumulative infiltration data or cumulative infiltration data in combination with additional information as described below. The objective function is defined as (Šimůnek and van Genuchten 1996)

$$\Phi(\beta, q_m) = \sum_{j=1}^{m} \left[\nu_j \sum_{i=1}^{n} w_i [q_j^*(t_i) - q_i, \beta)]^2 \right] \quad (8)$$

where m represents the different sets of measurements, such as the cumulative infiltration data or additional information, n_j is the number of measurements in a particular set, $q_j^*(t_i)$ are specific measurements at time t_i for the jth measurement set, β is the vector of optimized parameters (e.g., θ_r, θ_s, α, n, and K_s), $q_j(t_i, \beta)$ are the corresponding model predictions for the parameter vector β, and ν_j and w_i are weights associated with a particular measurement set or point, respectively. We assume for now that the weighting coefficients w_i in Eq (8) are equal to 1, that is, the variances of the errors inside of a particular measurement set are the same. The weighting coefficients ν_j are given by

$$\nu_j = \frac{1}{n_j \sigma_j^2} \quad (9)$$

thus defining the objective function as the average weighted squared deviation normalized by measurement variances σ_j^2.

Minimization of the objective function Φ is accomplished by using the Levenberg-Marquardt nonlinear minimization method (Marquardt 1963). The Levenberg-Marquardt method is a very effective method that has become a standard in nonlinear least-square fitting among soil scientists and hydrologists (van Genuchten 1981; Kool et al. 1985, 1987; van Dam et al. 1992, 1994). The method represents a compromise between the inverse-Hessian and steepest descent methods by using the steepest descent method when the objective function is far from its minimum, and switching to the inverse-Hessian method as the minimum is approached (Bard 1974). This switch is accomplished by multiplying the diagonal in the Hessian matrix (or its approximation $\boldsymbol{N} = \boldsymbol{J}^T\boldsymbol{J}$, where $\boldsymbol{J}$ is the Jacobian matrix whose elements are given by the sensitivity coefficients multiplied by a square root of the weight of a particular data point), sometimes called the curvature matrix, with $(1 + \lambda)$, where λ is a positive scalar. When λ is large, then the matrix is diagonally dominant resulting in the steepest descent method. On the other hand, when λ is zero, the inverse-Hessian method will result.

DATA GENERATION

The tension disc infiltration data used in this study were generated numerically using the HYDRUS-2D code (Šimůnek et al. 1996). The average parameter values for the loam soil textural group as estimated by Carsel and Parrish (1988) from analyses of a large number of soils were used during simulations. The soil hydraulic parameters of the hypothetical loam are as follows: $\theta_r = 0.078$, $\theta_s = 0.430$, $\alpha = 0.036\ \text{cm}^{-1}$, $n = 1.56$, and $K_s = 0.0002888\ \text{cm s}^{-1}$ (Carsel and Parrish 1988). The radius of the disc permeameter was assumed to be 10 cm. The initial pressure head or water content of the homogeneous and isotropic soil beneath the disc was taken as -500 cm or 0.1476, respectively. In practice, the initial pressure head or water content can vary with depth. A numerical code could easily account for such nonuniform initial conditions. Because the moisture front generally does not travel far from the disc (in our examples only about 12 cm), the constant initial condition was assumed to be adequate for the purpose of our study. The tension at the disc infiltrometer, h_0, was kept constant during 1 h and then increased twice to yield the following soil surface boundary condition:

$$h_0(t) = \begin{cases} -20\ \text{cm} & 0 < t \le 3600 \\ -10\ \text{cm} & 3600 < t \le 7200 \\ -3\ \text{cm} & 7200 < t \le 10800 \end{cases} \quad (10)$$

Our analysis involves the following steps and calculations. First, the known hypothetical soil hydraulic properties $\theta(h)$ and $K(h)$ were used in the direct problem to simulate a multiple tension disc infiltration event. This resulted in the computer-generated infiltration curve shown in Fig. 1. The finite element discretization was selected so that the mass balance error for the direct solutions always remained less than 0.05%. Infiltration rates were calculated as the sum of the actual nodal fluxes, Q_i [L^3T^{-1}], associated with nodes having prescribed Dirichlet boundary conditions representing the disc permeameter. The nodal fluxes could be calculated explicitly and accurately from the original finite element equations associated with these nodes (Šimůnek et al. 1996). The cumulative disc permeameter infiltration rate, $Q(t)$ [L^3], was calculated as follows

$$Q(t) = \int_{t_0}^{t} q(t)dt = \int_{t_0}^{t} \sum_{i=1}^{n} Q_i(t)dt \quad (11)$$

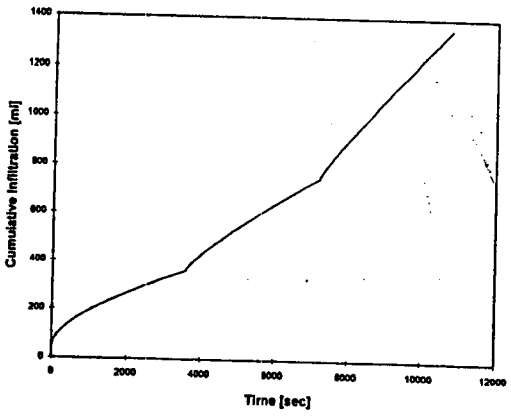

Fig. 1. Cumulative infiltration versus time for a hypothetical disc permeameter infiltration experiment with three consecutive supply pressure heads: $h_0(t = 0) = -20$ cm, $h_0(3600\ s) = -10$ cm, and $h_0(7200\ s) = -3$ cm.

where t_0 is the starting time of the experiment [T], $q(t)$ is the instantaneous infiltration rate [L^3T^{-1}], and n is the number of nodes representing the disc permeameter. Second, the numerically generated cumulative infiltration curve was discretized into discrete points distributed evenly over the curve. Third, the data obtained in steps 1 and 2 were used to calculate response surfaces of the objective function as a function of particular hydraulic parameters so as to determine possible uniqueness problems in the inverse procedure (Toorman et al. 1992). And fourth, the data obtained in steps 1 and 2 were used as input data for the inverse problem.

The third and fourth steps were repeated after including additional information in the objective function Φ. The additional information (final water content or the unsaturated hydraulic conductivity as estimated with Wooding's analytical solution) was combined with the primary measurement set (cumulative infiltration data) to evaluate whether additional data could substantially improve the error estimates on the parameters, including the goodness-of-fit. Sensitivities to the initial parameter estimates were also studied.

RESPONSE SURFACES AND INVERSE SOLUTIONS

We will concentrate on five different scenarios. First, we will analyze the objective function $\Phi(Q, h_i)$ defined solely by the cumulative infiltration data while assuming that the initial condition is given in terms of the pressure head. The last parameter in the argument in the notation of the objective function states how the initial condition was specified, whereas the other parameters specify what type of information was used in the objective function. In the second scenario, we will evaluate the behavior of the objective function $\Phi(Q, K, h_i)$, which, in addition to the infiltration data, now also contains two values of the unsaturated hydraulic conductivity as obtained by Wooding's (1968) analytical solution. The third scenario differs from the first one only by having initial condition specified in terms of the water content; hence, the objective function is now $\Phi(Q, \theta_i)$. Similarly, the objective function for the fourth scenario, $\Phi(Q, K, \theta_i)$, as for the second, will include information about the unsaturated hydraulic conductivity using Wooding's analysis. In the last scenario, we will analyze the objective function $\Phi(Q, \theta_f, \theta_i)$, which will include, in addition to the cumulative infiltration data, the final water content below the tension disc infiltrometer.

We calculated response surfaces for six parameter planes ($\alpha - n$, $\alpha - K_s$, $n - K_s$, $n - \theta_s$, $\alpha - \theta_s$, and $K_s - \theta_s$) for each of the data scenarios as described above. The response surfaces were calculated on a rectangular grid, with parameter values given in Table 1. Each parameter domain was discretized into 30 discrete points, resulting in 900 grid points for each response surface. This means that we carried out 27,000 (= 5 scenarios × 6 parameter planes × 900 grid points) direct solutions of the multiple tension disc infiltration experiment.

Analysis of Objective Function $\Phi(Q, h_i)$

Figure 2 shows response surfaces for the objective function $\Phi(Q, h_i)$ based on the multiple tension cumulative infiltration curve for the initial condition given by Eq (3). Figures 2a, b, and c show response surfaces quantitatively similar to the response surfaces calculated for the objective function based on one tension cumulative infiltration curve (Šimůnek and van Genuchten 1996).

TABLE 1

Grid spacings used for the parameter planes of the hypothetical disc permeameter infiltration experiment

Parameter	Lower parameter value	Parameter step value	Upper parameter value
α[cm^{-1}]	0.002	0.002	0.06
n[−]	1.0333	0.03333	2.0
K_s[$cm\ s^{-1}$]	0.00001	0.00002	0.00006
θ_s[−]	0.347	0.007	0.550

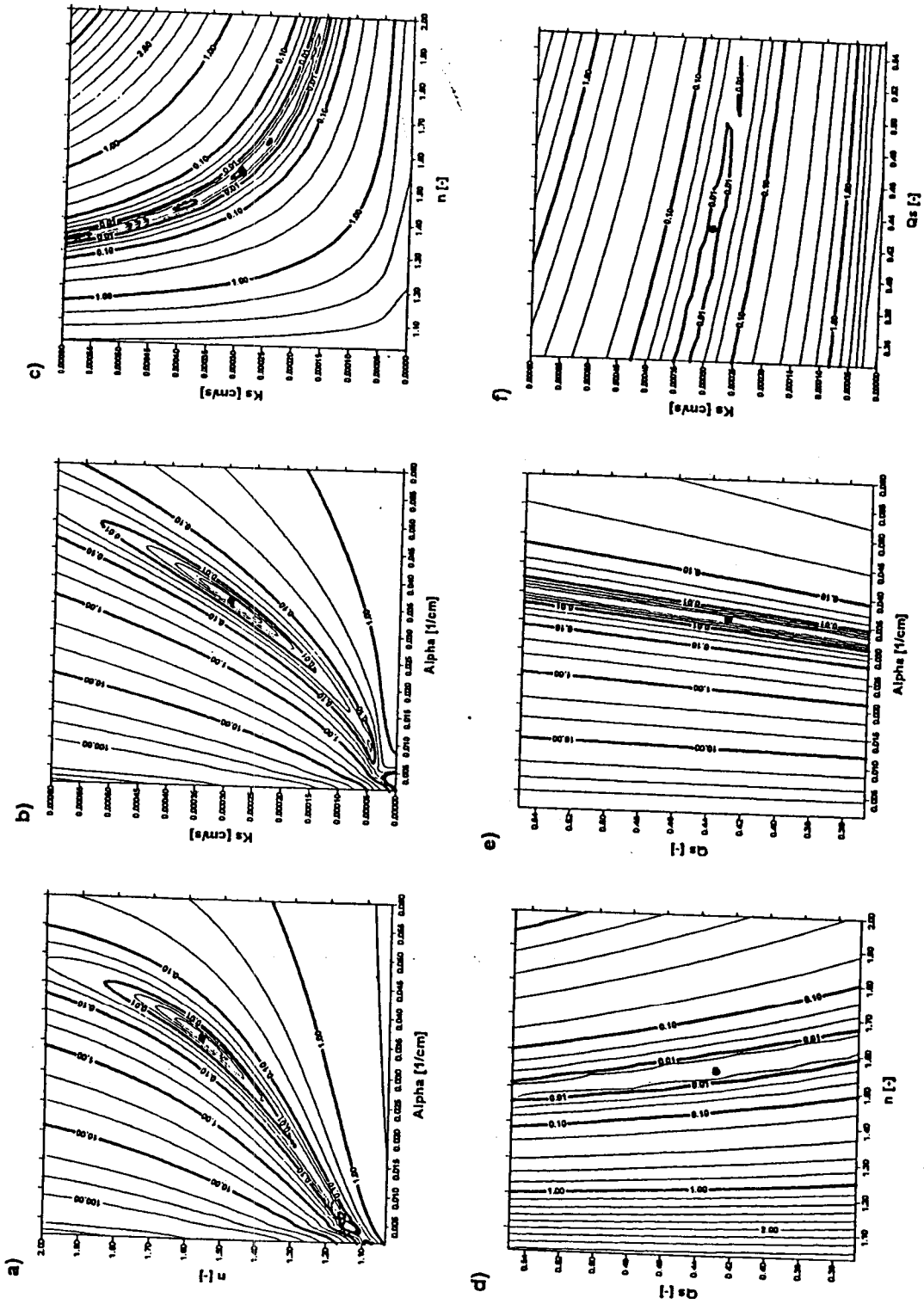

Fig. 2. Contours of the objective function $\Phi(Q, h_i)$ for cumulative infiltration. Results are plotted in the a) $\alpha - n$, b) $\alpha - K_s$, c) $n - K_s$, d) $n - \theta_r$, e) $\alpha - \theta_r$, and f) $\theta_s - K_s$ parameter planes. The initial condition is given in terms of the pressure head.

Although the global minima in the $\alpha - n$ and $\alpha - K_s$ parameter planes are well defined, parameter estimation from the data associated with this objective function would probably be unsuccessful because there is no clearly defined minimum in the $n - K_s$ parameter plane (Fig. 2c). If, on the other hand, K_s were known, this approach would lead to a successful determination of α and n. The response surface in the $\alpha - n$ parameter plane (Fig. 2a) shows several local minima as well as a global minimum, probably the result of small numerical inaccuracies in this extreme end of the parameter plane. Figure 2c shows a hyperbolic valley with a nearly identical minimum along the bottom of the valley. This result means that, similar to a single tension experiment (Šimůnek and van Genuchten 1996), any combination of parameter values in this valley will yield almost identical cumulative infiltration curves. This feature suggests that the parameters n and K_s can not be estimated simultaneously from an objective function of the form $\Phi(Q, h_i)$. Figures 2d, 2e, and 2f also show that there is no clearly defined minimum with respect to θ_s. The contour lines in all three parameter planes are almost parallel to the θ_s axis.

To confirm the above results obtained by analyzing response surfaces, we used the Levenberg-Marquardt optimization method to numerically find the global minimum of the objective function $\Phi(Q, h_i)$. The results of the inverse solutions are summarized in Table 2 for the first three cases. Particular cases differ with respect to the number of optimized parameters; for each case, we started with three sets of different initial estimates for the hydraulic parameters α and n.

For the first optimization case, we optimized only the shape factor α and n and fixed the other parameters at their true value. The optimization procedure converged in two runs to the global minimum but stopped at a local minimum for the third run (see Fig. 2a). In the second case we optimized the saturated hydraulic conductivity, K_s, in addition to parameters α and n. The program again converged to the true values of optimized parameters in two out of three runs. While this result may seem to contradict our conclusion drawn from analysis of the response surfaces in Fig. 2c, in reality it reflects the robustness of the optimization algorithm. Although the hyperbolic valley in Fig. 2c has very small Φ values, the values are still positive. The value of the objective function should be zero only for the true parameters and a robust optimization algorithm should find this point providing that the objective function is convex. Nevertheless, in case of real data, which always contain measurement errors, or with hy-

TABLE 2

Results of inverse solutions for cases where the initial condition is given in terms of the pressure head h_i, i.e., for objective functions $\Phi(Q, h_i)$ and $\Phi(Q, K, h_i)$

Case	Objective function type	Initial estimates				Final estimates				
		α	n	K_s	θ_s	α	n	K_s	θ_s	Φ
1a	$\Phi(Q, h_i)$	0.010	1.8000	0.00029	0.430	0.03623	1.56379			0.6144e-05*
b		0.015	2.3940	0.00029	0.430	0.03623	1.56385			0.613e-05*
c		0.003	1.4364	0.00029	0.430	0.00555	1.14012			0.1653e-01
2a	$\Phi(Q, h_i)$	0.010	1.8000	0.00010	0.430	0.03628	1.55436	0.00030		0.5764e-05*
b		0.015	2.3940	0.00010	0.430	0.03628	1.43640	0.00030		0.5769e-05*
c		0.003	1.4364	0.00010	0.430	0.00918	1.11831	0.00065		0.1111e-01
3a	$\Phi(Q, h_i)$	0.010	1.8000	0.00010	0.450	0.03637	1.55207	0.00030	0.43157	0.5697e-05*
b		0.015	2.3940	0.00010	0.450	0.03504	1.73315	0.00020	0.42311	0.7133e-04
c		0.003	1.4364	0.00010	0.450	0.03640	1.54922	0.00030	0.43201	0.5680e-05*
4a	$\Phi(Q, K, h_i)$	0.010	1.8000	0.00029	0.430	0.03882	1.64058			0.3376e-02
b		0.015	2.3940	0.00029	0.430	0.03882	1.64058			0.3376e-02
c		0.003	1.4364	0.00029	0.430	0.03882	1.64058			0.3376e-02
5a	$\Phi(Q, K, h_i)$	0.010	1.8000	0.00010	0.430	0.03865	1.84974	0.00021		0.2054e-02
b		0.015	2.3940	0.00010	0.430	0.03864	1.85042	0.00021		0.2054e-02
c		0.003	1.4364	0.00010	0.430	0.03426	1.19380	0.00140		0.8472e-03
6a	$\Phi(Q, K, h_i)$	0.010	1.8000	0.00010	0.450	0.03561	1.55018	0.00032	0.37100	0.4492e-03
b		0.015	2.3940	0.00010	0.450	0.03587	1.58672	0.00030	0.37412	0.5146e-03
c		0.003	1.4364	0.00010	0.450	0.03496	1.44689	0.00041	0.36650	0.3749e-03
Real Parameters						0.036	1.56	0.00029	0.430	

* = Successful runs.

pothetical errors superimposed on the exact solution, such optimization would apparently be unsuccessful. The same analysis holds for the third case involving four optimized parameters.

Analysis of Objective Function $\phi(Q, K, h_i)$: Combination of Cumulative Infiltration Data with Wooding's Analytical Solution

If the objective function of the type $\Phi(Q, h_i)$ does not contain enough information, the question is what easily measured additional data could be added to ensure convergence in the inverse solution. The scenario wherein the final water content below the tension disc θ_f is added to the objective function is considered later. Here we consider the intermediate step of using more information embedded in the infiltration curve. In the traditional analysis of the tension disc experiment, based on the Wooding's (1968) analytical solution, one needs two steady-state fluxes at different tensions (Ankeny et al. 1991) to derive the saturated hydraulic conductivity K_s and the sorptivity number α^* in Gardner's exponential model (Gardner 1958) of the unsaturated hydraulic conductivity

$$K(h) = K_s \exp(\alpha^* h) \tag{12}$$

Wooding's (1968) solution for infiltration from a circular source with a constant pressure head at the soil surface and with the unsaturated hydraulic conductivity described by Eq (12), is given by

$$Q(h_0) = \left[\pi r_0^2 + \frac{4r_0}{\alpha^*}\right] K(h_0) \tag{13}$$

where Q is the steady-state infiltration rate [L^3T^{-1}], r_0 is the radius of the disc [L], h_0 is the wetting pressure head [L], and $K(h_0)$ is the unsaturated hydraulic conductivity [LT^{-1}] at pressure head h_0. The first term on the right side represents the effects of gravitational forces, and the second term represents the effects of capillary forces. The theory for obtaining the unsaturated hydraulic conductivity in the middle of the interval between two successively applied pressure heads was described previously by Ankeny et al. (1991), Reynolds and Elrick (1991), and Jarvis and Messing (1995), among others. The approach assumes that the sorptivity number α^* in Gardner's exponential model Eq. (12) is constant in the interval between two adjacent supply pressure heads, such that

$$\alpha^*_{i+1/2} = \frac{\ln \dfrac{Q_i}{Q_{i+1}}}{h_i - h_{i+1}} \qquad i = 1,\ldots, n-1 \tag{14}$$

where n is the number of infiltration tensions used and where the subscript 1/2 on α^* is used to indicate that α^* is estimated in the middle of two adjacent supply pressure heads: $h_{i+1/2} = (h_i + h_{i+1})/2$. The unsaturated hydraulic conductivity at pressure head $h_{i+1/2}$ is then calculated as

$$K_{i+1/2} = \frac{Q_{i+1/2}}{\pi r^2 + \dfrac{4r}{\alpha^*_{i+1/2}}} \qquad i = 1,\ldots,n-1 \tag{15}$$

in which the estimated infiltration rate $Q_{i+1/2}$ at the middle of two adjacent supply pressure heads $h_{i+1/2}$ is calculated as a geometric mean of the actual infiltration rates Q_i and Q_{i+1}

$$Q_{i+1/2} = \exp\frac{\ln Q_i + \ln Q_{i+1}}{2} \qquad i = 1,\ldots,n-1 \tag{16}$$

The saturated hydraulic conductivity K_s can be calculated from Eq (12) using known values of $h_{i+1/2}$, $K_{i+1/2}$ and $\alpha^*_{i+1/2}$ as follows

$$K_s = \frac{K_{i+1/2}}{\exp(\alpha^*_{i+1/2} h_{i+1/2})} \tag{17}$$

The objective function $\Phi(Q, K, h_i)$ can be defined as the sum of the objective function based on the multiple tension cumulative curve $\Phi(Q, h_i)$ and the information obtained from Wooding's analytical solution. There are several possibile ways to define the objective function $\Phi(Q, K, h_i)$: using only the unsaturated hydraulic conductivities $K_{i+1/2}$, using the calculated saturated hydraulic conductivity K_s, or using both saturated and unsaturated hydraulic conductivities simultaneously. Although we ran all three options, we will show below only the response surfaces for the combination of multiple tension cumulative infiltration data and two values of the unsaturated hydraulic conductivities $K_{i+1/2}$.

The hypothetical data were generated using van Genuchten's (1980) prediction of the unsaturated hydraulic conductivity (Eq.(7)). By using Wooding's analytical solution, we assume that the unsaturated hydraulic conductivity function within the interval between two adjacent supply pressure heads can be interpolated accurately by means of the exponential function (Eq.(12)). Because the interval between two adjacent supply pressure heads, h_i and h_{i+1}, is relatively small, in our case 10 and 7 cm, the exponential assumption seems acceptable. From our numerical simulation, we estimated the unsaturated hydraulic conductivities to be $K(h = -6.5\text{ cm}) = 0.0001025\text{ cm s}^{-1}$

and $K(h = -15\text{ cm}) = 0.0000412\text{ cm s}^{-1}$. The true values of the unsaturated hydraulic conductivities were $K(h = -6.5\text{ cm}) = 0.0000929\text{ cm s}^{-1}$ and $K(h = -15\text{ cm}) = 0.0000372\text{ cm s}^{-1}$, i.e., the Wooding's analytical solution produced hydraulic conductivities that differed only by about 10% from the true values. This indicates that traditional Wooding/Gardner analysis of tension infiltrometer is quite good and can be used as a first approximation for parameter estimation methods.

Figure 3 shows the response surfaces for the objective function $\Phi(Q, K, h_i)$ based on a combination of multiple tension cumulative infiltration data with unsaturated hydraulic conductivities obtained with Wooding's analytical solution. The minima in the $\alpha - n$ and $\alpha - K_s$ parameter planes are better defined than in Figs. 2a and b; however, there is now a small shift from the true values. The global minimum in the $\alpha - n$ parameter plane shifted from the true value at (0.036, 1.56) to about (0.039, 1.64), which represents errors in the α and n parameters of about 7% and 5%, respectively. Similarly, the shift in the $\alpha - K_s$ parameter plane from the true value (0.036, 0.0002889) to about (0.0385, 0.00033) represents errors of about 7% and 14% in α and K_s, respectively. These errors may be acceptable for most practical purposes. Note that the additional local minima, as shown in Fig. 2a, disappeared after introducing the information about the unsaturated hydraulic conductivities (Fig. 3a). The response surface in the $n - K_s$ parameter plane still displays a hyperbolic valley with no apparent minimum. In contrast to the response surfaces in Figs. 2d, e, and f for cases involving the saturated water content, θ_s, the response surfaces shown in Fig. 3 now exhibit reasonably well defined minima. These minima, however, are shifted from the true value of the saturated water content by about 0.006.

The numerical inversions (Cases 4, 5, and 6 in Table 2) again confirm our conclusions from the analysis of response surfaces. The optimization method found the minimum easily when only two shape factors, α and n, were sought for any initial estimate of their values. The results of the optimization confirms the shift of the optimized values of the parameters α and n from their true values as seen in Fig. 3a. Because objective function $\Phi(Q, K, h_i)$, unlike $\Phi(Q, h_i)$, did not display any local minimum in addition to the global minimum for the true parameter values, all three optimization runs converged to the same values of the optimized parameters.

The objective function $\Phi(Q, K, h_i)$ does not have a zero value, even for the true parameters, since we included in its definition two values of the unsaturated hydraulic conductivity. Another reason for the shift is the assumption of Gardner's exponential equation for the hydraulic conductivity function. This error depends on the extent to which the exponential function can or cannot approximate van Genuchten's hydraulic conductivity function. In practical situations, one cannot foresee a priori which hydraulic conductivity model should be the more appropriate one (Russo 1988), and inclusion of the unsaturated hydraulic conductivity values calculated with Wooding's analytical solution could, in fact, decrease the error invoked by assuming validity of van Genuchten's hydraulic conductivity function.

Inspection of Table 2 shows that one of the minima found when the saturated hydraulic conductivity K_s was estimated (Case 5c) is located far outside the interval for which we calculated the response surfaces. When all four parameters were fitted simultaneously, the final estimates remained relatively close to the true parameter values, with the exception of the saturated water content, θ_s, which, in all three cases, was underestimated by about 0.006. This shift was also clearly demonstrated in Figs 3d, e, and f.

Analysis of Objective Function $\Phi(Q, \theta_i)$.

Until now, we assumed that the initial condition was known and given in terms of the pressure head (Eq. (3)). Following, we define the initial condition in terms of the water content:

$$\theta(r, z, t) = \theta_i \qquad t = 0 \qquad (18)$$

where θ_i is the initial water content, assumed to be constant here. Specifying the initial condition in terms of the water content has a profound effect on the response surfaces (Fig. 4). Minima are now well defined in five ($\alpha - n$, $\alpha - K_s$, $n - K_s$, $n - \theta_s$, and $K_s - \theta_s$) of the six parameter planes. Several local minima, as shown in Fig. 2a, have also disappeared (Fig. 4a). Note that the response surface in the parameter plane $n - K_s$ (Fig. 4c) now has a well defined minimum compared with the cases shown in Figs. 2c and 3c. The prospect of estimating n and K_s simultaneously from cumulative infiltration curves for both single (Šimůnek and van Genuchten 1996) and multiple (Figs. 2c and 3c) supply pressure heads when the initial condition is given in terms of the pressure head was always found to be negative. The results in Fig. 4 are much better in this respect; still, the lack of a minimum on the response surface in the $\alpha - \theta_s$ parameter plane shows that the saturated water content θ_s cannot be estimated simultaneously

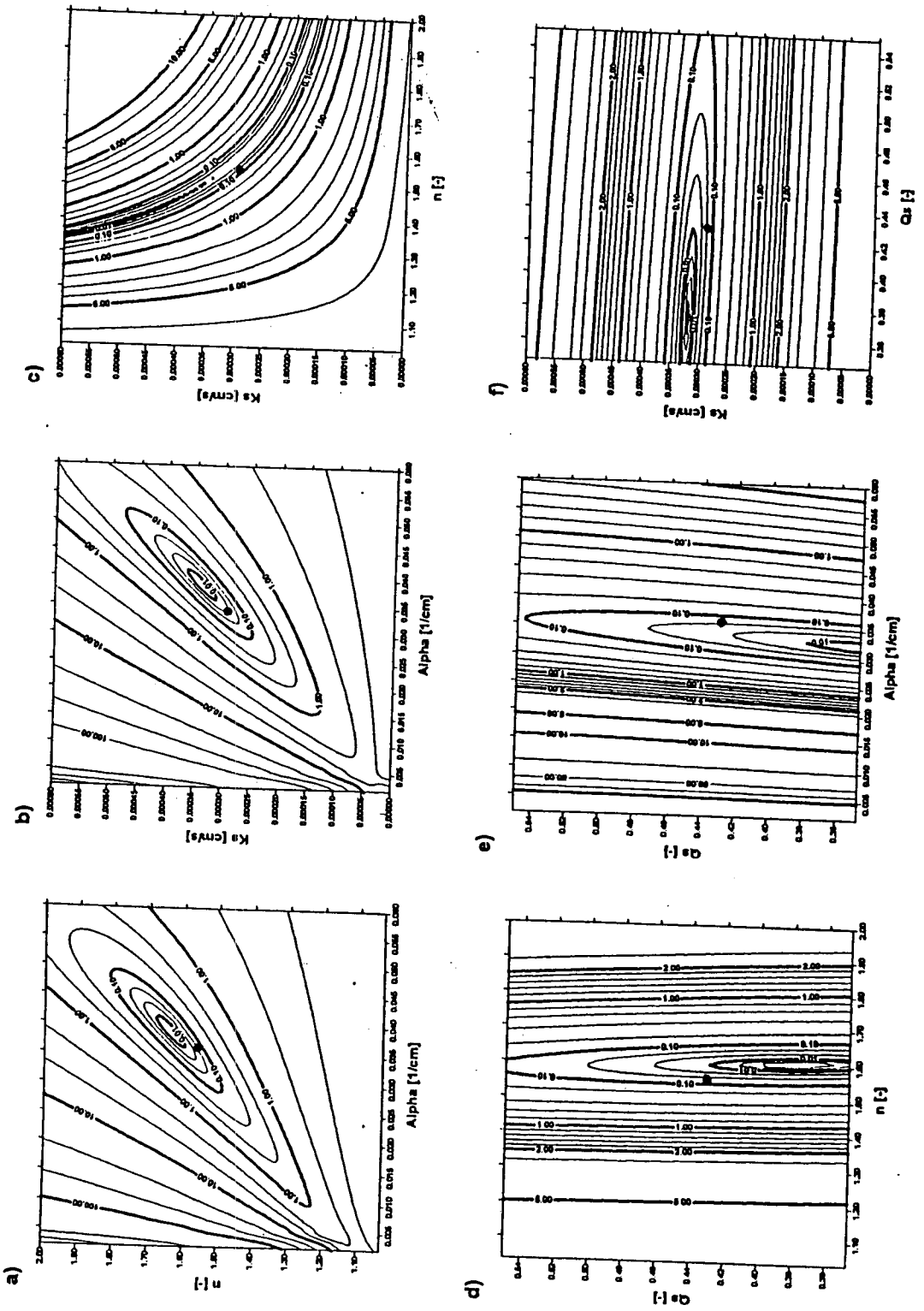

Fig. 3. Contours of the objective function $\Phi(Q, K, h_i)$ for cumulative infiltration, with the unsaturated hydraulic conductivities obtained using Wooding's 1968. analytical solution. Results are plotted in the a) $\alpha - n$, b) $\alpha - K_s$, and c) $n - K_s$, d) $n - \theta_s$, e) $\alpha - \theta_s$, and f) $\theta_s - K_s$ parameter planes. The initial condition is given in terms of the pressure head.

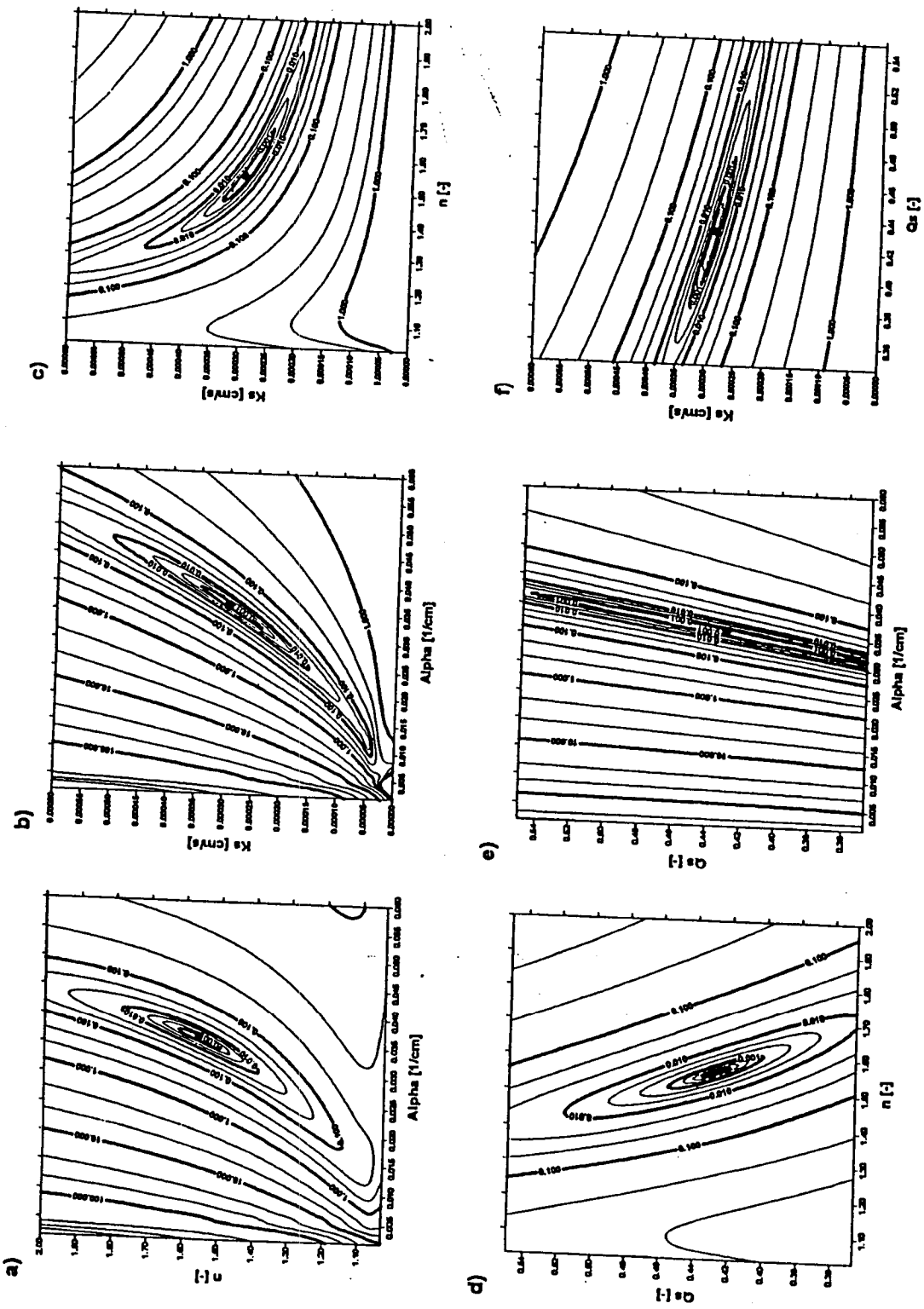

Fig. 4. Contours of the objective function $\Phi(Q, \theta_i)$ for cumulative infiltration. Results are plotted in the a) $\alpha - n$, b) $\alpha - K_s$, c) $n - K_s$, d) $n - \theta_s$, e) $\alpha - \theta_s$, and f) $\theta_s - K_s$ parameter planes. The initial condition is given in terms of the water content.

with other parameters when using an objective function of the type $\Phi(Q, \theta_i)$.

Numerical optimization of soil hydraulic parameters using the objective function $\Phi(Q, \theta_i)$ was successful in all cases (Table 3, Cases 1, 2, and 3). Although Figure 4e did not show a clearly defined minimum, and the contour lines exhibited a long narrow valley almost parallel with the θ_s axis, the numerical inversion easily found the global minimum. This result can be explained in a way similar to that of $\theta(Q, h_i)$. The global minimum of the objective function for the hypothetical case with no superimposed artificial errors has a value equal to zero, and any robust algorithm should be able to find its position providing there are no additional local minima in parameter space. However, in real situations, where many errors are involved (such as instrumental and recording errors, calibration errors, or errors associated with the invoked theoretical model) (Bard 1974; Press et al. 1989; Russo et al. 1991; McLaughlin and Townley 1996), it would be difficult to determine the saturated water content θ_s from an objective function of the form $\theta(Q, \theta_i)$.

Analysis of Objective Function $\Phi(Q, K, \theta_i)$: Combination of Cumulative Infiltration Data with Wooding's Analytical Solution.

Similar to the above analysis, we will combine the objective function $\Phi(Q, \theta_i)$ with two values of the unsaturated hydraulic conductivity $K_{i+1/2}$ as estimated using Wooding's analytical solution (Eq. (13)) to obtain the objective function $\Phi(Q, K, \theta_i)$. The response surfaces for the objective function $\Phi(Q, K, \theta_i)$ are shown in Fig. 5. As with Fig. 3, inclusion of the estimated unsaturated hydraulic conductivities resulted in a slight deviation of the minima from the true values. The global minimum in the $\alpha - n$ parameter plane shifted from the true value of (0.036, 1.56) to about

TABLE 3

Results of inverse solutions for cases where the initial condition is given in terms of the water content θ_i, i.e., for objective functions $\Phi(Q, \theta_i)$, $\Phi(Q, K, \theta_i)$, and $\Phi(Q, \theta_f, \theta_i)$

Case	Objective function type	Initial estimates				Final estimates				Φ
		α	n	K_s	θ_s	α	n	K_s	θ_s	
1a	$\Phi(Q, \theta_i)$	0.010	1.8000	0.00029	0.430	0.03610	1.56236			0.6336e-05*
b		0.015	2.3940	0.00029	0.430	0.03610	1.56237			0.6339e-05*
c		0.003	1.4364	0.00029	0.430	0.03610	1.56237			0.6337e-05*
2a	$\Phi(Q, \theta_i)$	0.010	1.8000	0.00010	0.430	0.03642	1.55371	0.00030		0.5755e-05*
b		0.015	2.3940	0.00010	0.430	0.03643	1.55328	0.00030		0.5712e-05*
c		0.003	1.4364	0.00010	0.430	0.03638	1.55438	0.00030		0.5736e-05*
3a	$\Phi(Q, \theta_i)$	0.010	1.8000	0.00010	0.450	0.03616	1.58015	0.00028	0.43841	0.8382e-05*
b		0.015	2.3940	0.00010	0.450	0.03638	1.55267	0.00030	0.42905	0.5661e-05*
c		0.003	1.4364	0.00010	0.450	0.03641	1.55094	0.00030	0.42874	0.5681e-05*
4a	$\Phi(Q, K, \theta_i)$	0.010	1.8000	0.00029	0.430	0.03741	1.62434			0.1436e-02
b		0.015	2.3940	0.00029	0.430	0.03741	1.62435			0.1436e-02
c		0.003	1.4364	0.00029	0.430	0.03740	1.62423			0.1436e-02
5a	$\Phi(Q, K, \theta_i)$	0.010	1.8000	0.00010	0.430	0.03685	1.65710	0.00027		0.1177e-02
b		0.015	2.3940	0.00010	0.430	0.03680	1.65978	0.00027		0.1179e-02
c		0.003	1.4364	0.00010	0.430	0.03681	1.65933	0.00027		0.1179e-02
6a	$\Phi(Q, K, \theta_i)$	0.010	1.8000	0.00010	0.450	0.03481	1.40849	0.00047	0.33763	0.2770e-03
b		0.015	2.3940	0.00010	0.450	0.03531	1.49542	0.00037	0.36846	0.3880e-03
c		0.003	1.4364	0.00010	0.450	0.03466	1.38683	0.00050	0.32954	0.2777e-03
7a	$\Phi(Q, \theta_f, \theta_i)$	0.010	1.8000	0.00029	0.430	0.03611	1.56248			0.6394e-05*
b		0.015	2.3940	0.00029	0.430	0.03611	1.56239			0.6371e-05*
c		0.003	1.4364	0.00029	0.430	0.03610	1.56237			0.6359e-05*
8a	$\Phi(Q, \theta_f, \theta_i)$	0.010	1.8000	0.00010	0.430	0.03641	1.55398	0.00030		0.5750e-05*
b		0.015	2.3940	0.00010	0.430	0.03644	1.55240	0.00030		0.5791e-05*
c		0.003	1.4364	0.00010	0.430	0.03644	1.55240	0.00030		0.5791e-05*
9a	$\Phi(Q, \theta_f, \theta_i)$	0.010	1.8000	0.00010	0.450	0.03644	1.55310	0.00030	0.42991	0.5775e-05*
b		0.015	2.3940	0.00010	0.450	0.03639	1.55426	0.00030	0.42991	0.5713e-05*
c		0.003	1.4364	0.00010	0.450	0.03641	1.55356	0.00030	0.42991	0.5745e-05*
Real parameters						0.036	1.56	0.00029	0.430	

* = Successful runs.

(0.0374, 1.624), which represents errors in α and n of about 4%. As well, the shift in the $\alpha - K_s$ parameter plane from the true value of (0.036, 0.0002889) to about (0.0385, 0.00033) represents errors of about 7% and 14% in α and K_s, respectively. Again, we believe that these error values are acceptable for most practical purposes. The biggest shift in the minima of objective function $\Phi(Q, K, \theta_i)$ occurs when θ_s is involved. The biggest shift in θ_s occurs in the $\alpha - \theta_s$ parameter plane (Fig. 5d) where it represents an error of about 0.007. This error is still an improvement when compared with the previous case where the minimum of the objective function $\Phi(Q, \theta_i)$ in the parameter plane $\alpha - \theta_s$ was visually unidentifiable.

The results of our inverse solutions (Table 3, Cases 4, 5, and 6) are consistent with the above analyses using response surfaces. When only two shape parameters, α and n, in addition to K_s, were identified simultaneously, the results exhibited a shift from the true values of the optimized parameters. On the other hand, when all four parameters including θ_s were optimized simultaneously, the results yielded an unacceptable error in θ_s.

Analysis of Objective Function $\Phi(Q, \theta_f, \theta_i)$: Combination of Cumulative Infiltration Data with Final Water Content.

One other variable that may be measured easily is the water content associated with the final supply pressure head at the end of the experiment. After removal of the tension disc infiltrometer, a soil sample could be taken directly below the disc and the actual water content measured in the laboratory. This information can be included to the earlier objective function $\Phi(Q, \theta_i)$ to obtain the new function $\Phi(Q, \theta_f, \theta_i)$, where θ_f is the water content (0.426) at the final supply pressure head h_f (= −3 cm). Figure 6 shows the response surfaces of the objective function $\Phi(Q, \theta_f, \theta_i)$ in all six parameter planes. The response surfaces now exhibit a very well defined global minimum in all six parameter planes ($\alpha - n$, $\alpha - K_s$, $n - K_s$, $\alpha - \theta_s$, $n - \theta_s$, and $K_s - \theta_s$). The weighting coefficient ν_j for the water content θ_f at the final supply pressure head h_f was set equal to one. Definition of the global minima in the three parameter planes involving θ_s (Fig. 6d, e, and f) could be somewhat improved by increasing the weighting coefficient ν_j for this point of the retention curve. The inverse solutions for all cases (Table 3, Cases 7, 8, and 9) yielded nearly exactly the true values. Clearly, this scenario with an objective function $\Phi(Q, \theta_f, \theta_i)$ involving measurement of the cumulative infiltration, and the initial and final water contents, represents the most promising case for experimental evaluation.

MEASUREMENT ERRORS

Until now, we used exact error-free data for both the calculation of response surfaces and for inverse solutions. In real situations, experimental data are subject to instrumentation, calibration, and other errors. Such errors tend to destabilize the inverse solution by creating several local minima, or by shifting the location of the global minimum of the objective function in parameter space. To assess the stability of the inverse solution we superimpose a random measurement error on the infiltration data and a deterministic error on both the initial and final water contents. The random mean error in the infiltration data, as caused by the instrumentation and reading errors, was assumed to be zero with a variance equal to 0.53. We determined this value of the variance by analyzing the observed cumulative infiltration curves (unpublished data) obtained using the automated tension disc permeameter of Ankeny et al. (1988). A deterministic error of 0.02 was added or subtracted from both the initial and final water contents.

Table 4 shows the results for the inverse solutions for eight different scenarios. In the first two scenarios, only the cumulative infiltration curve was made subject to a random error, whereas the final water content was assumed to be either not measured, yielding objective function $\Phi(Q^*, \theta_i)$, or measured without errors, leading to objective function $\Phi(Q^*, \theta_f, \theta_i)$. The third and sixth scenarios again considered a random error in the infiltration data, but they now also considered deterministic errors (+0.02 or −0.02) in the initial water content, resulting in objective functions $\Phi(Q^*, \theta_i + 0.02)$ and $\Phi(Q^*, \theta_{i-0.02} - 0.02)$, respectively. The last four scenarios also considered the deterministic error in the final water content, resulting in objective functions $\Phi(Q^*, \theta_f - 0.02, \theta_i + 0.02)$, $\Phi(Q^*, \theta_f + 0.02, \theta_i + 0.02)$, $\Phi(Q^*, \theta_f - 0.02, \theta_i - 0.02)$, and $\Phi(Q^*, \theta_f + 0.02, \theta_i - 0.02)$. Each scenario, similar to the error-free data, was run with two, three, and four optimized parameters and with three different initial estimates of the α and n parameters (the same as in Tables 2 and 3). In Table 4, we do not give the results for all three runs with the different initial estimates, but rather only those cases that yielded the smallest value of objective function and the number of runs that resulted in this solution.

The results in Table 4 suggest that superimposition of measurement errors on the error-free data resulted in only small deviations from the true

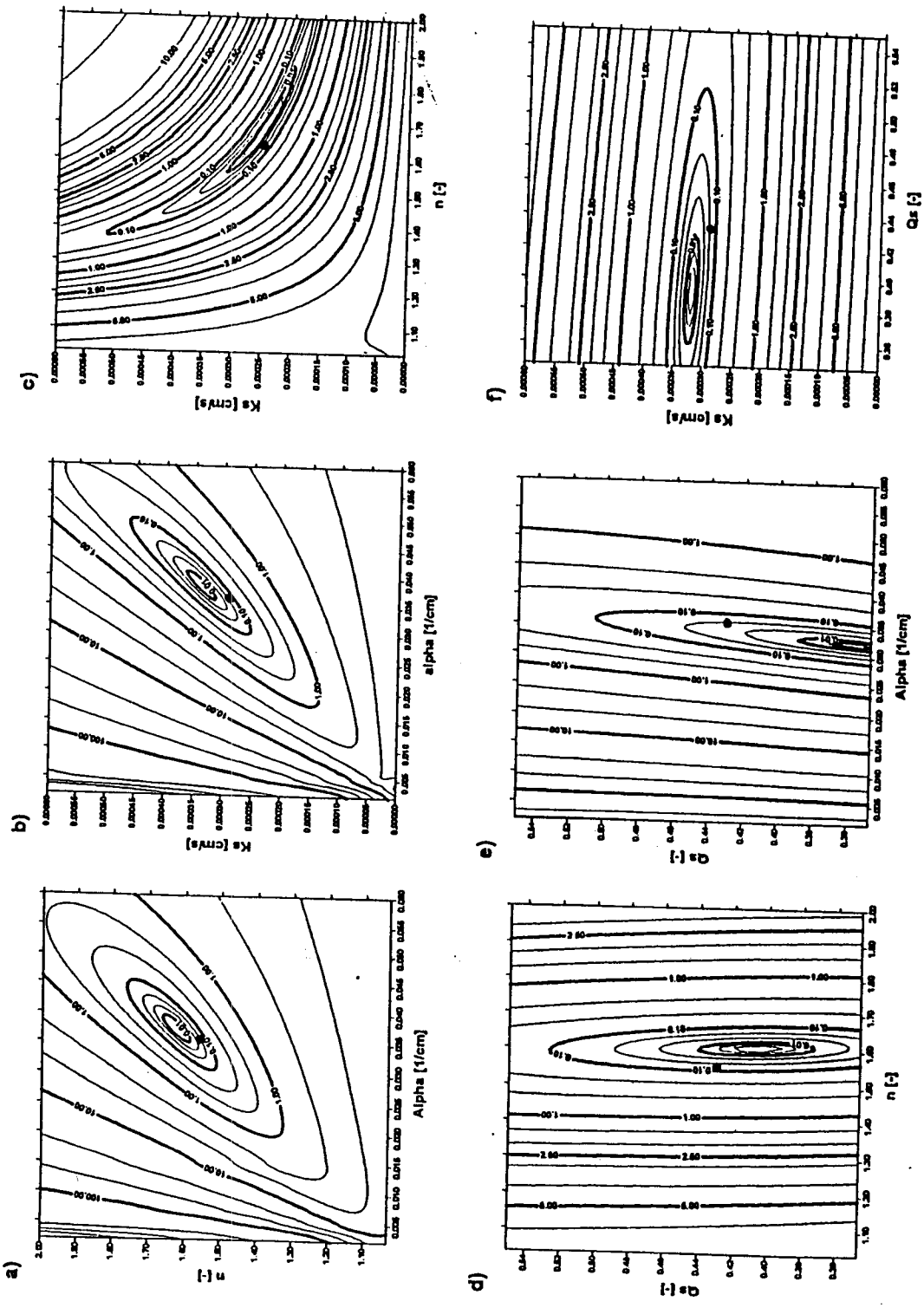

Fig. 5. Contours of the objective function $\Phi(Q, K, \theta_s)$ for cumulative infiltration, with the unsaturated hydraulic conductivities obtained using Wooding's (1968) analytical solution. Results are plotted in the a) $\alpha - n$, b) $\alpha - K_s$, c) $n - K_s$, d) $n - \theta_s$, e) $\alpha - \theta_s$, and f) $\theta_s - K_s$ parameter planes. The initial condition is given in terms of the water content.

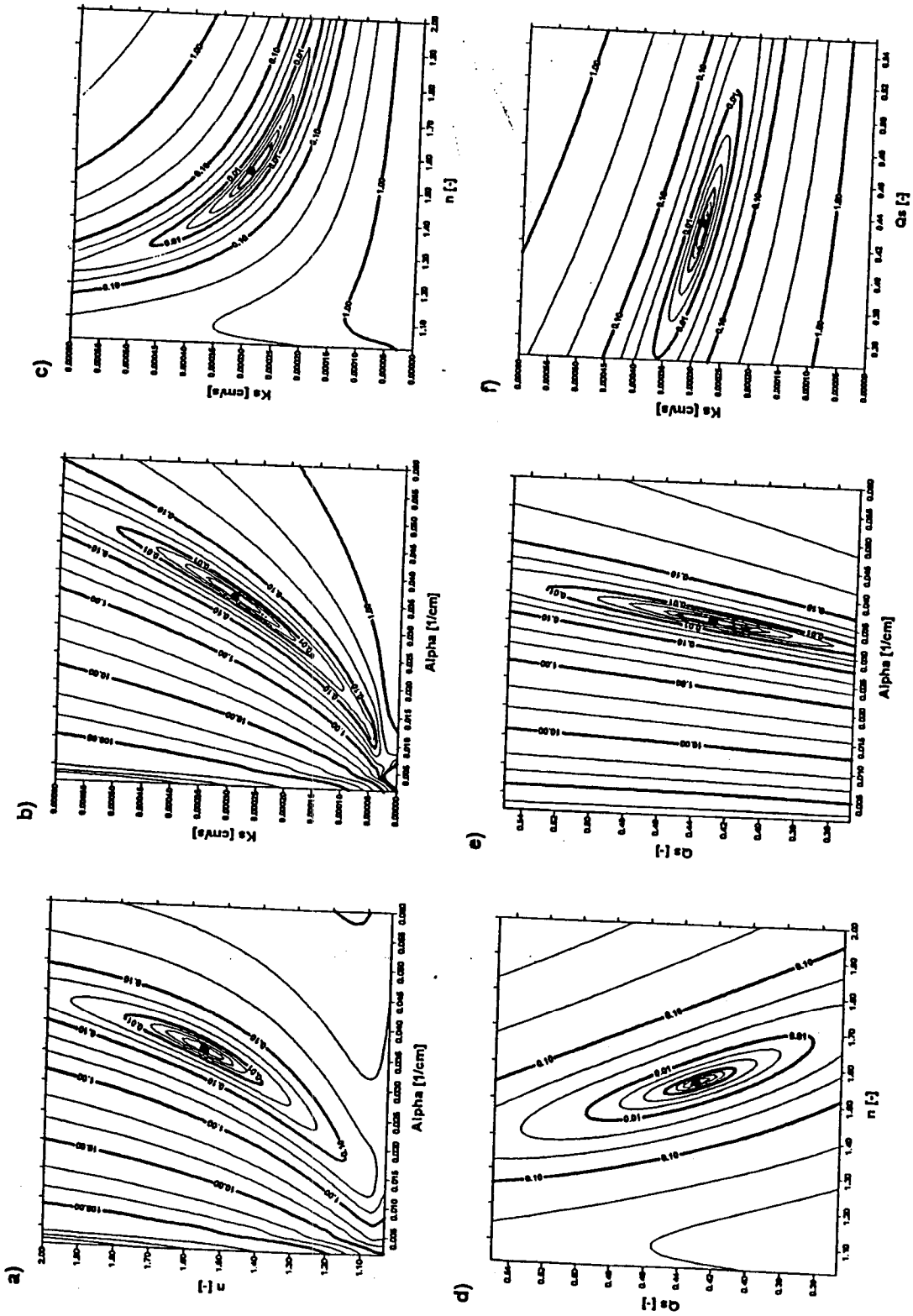

Fig. 6. Contours of the objective function $\Phi(Q, \theta_r, \theta_s)$ for cumulative infiltration assuming knowledge of the final water content below the tension disc infiltrometer. Results are plotted in the a) $\alpha - n$, b) $\alpha - K_s$, c) $n - K_s$, d) $\alpha - \theta_s$, e) $n - \theta_s$, and f) $\theta_s - K_s$ parameter planes. The initial condition is given in terms of the water content.

TABLE 4

Results of inverse solutions for cases with superimposed random or deterministic errors

Scenario	Objective function type	Final estimates				Φ	Number of successful runs
		α	n	K_s	θ_s		
1a	$\Phi(Q^*, \theta_i)$	0.03598	1.55958			0.6170e-05	3
b		0.03600	1.55863	0.00029		0.6166e-05	3
c		0.03595	1.55546	0.00029	0.42793	0.6120e-05	2
2a	$\Phi(Q^*, \theta_f, \theta_i)$	0.03598	1.55950			0.6197e-05	3
b		0.03600	1.55863	0.00029		0.6189e-05	3
c		0.03596	1.55958	0.00029	0.42981	0.6157e-05	3
3a	$\Phi(Q^*, \theta_i - 0.02)$	0.03812	1.57955			0.4285e-04	3
b		0.03649	1.63537	0.00025		0.1771e-04	3
c		0.03581	1.58685	0.00028	0.39838	0.6675e-04	3
4a	$\Phi(Q^*, \theta_f - 0.02, \theta_i - 0.02)$	0.03812	1.57960			0.4384e-03	3
b		0.03712	1.61107	0.00026		0.4291e-03	3
c		0.03605	1.60430	0.00027	0.40934	0.8007e-05	2
5a	$\Phi(Q^*, \theta_f + 0.02, \theta_i - 0.002)$	0.03812	1.57958			0.4474e-03	3
b		0.03598	1.65558	0.00024		0.3978e-03	3
c		0.03683	1.66501	0.00023	0.44919	0.3480e-04	3
6a	$\Phi(Q^*, \theta_i + 0.02)$	0.03391	1.54011			0.3715e-04	3
b		0.03557	1.48847	0.00034		0.1411e-04	3
c		0.03606	1.52869	0.00031	0.45575	0.7050e-05	2
7a	$\Phi(Q^*, \theta_f - 0.02, \theta_i + 0.02)$	0.03392	1.54025			0.4541e-03	3
b		0.03636	1.54025	0.00037		0.4087e-03	3
c		0.03514	1.46847	0.00038	0.40992	0.2985e-04	2
8a	$\Phi(Q^*, \theta_f + 0.02, \theta_i + 0.02)$	0.03391	1.54012			0.4207e-03	3
b		0.03487	1.50898	0.00032		0.4118e-03	3
c		0.03592	1.52158	0.00031	0.45027	0.7298e-05	2
Real parameters		0.036	1.56	0.00029	0.430		

parameters. The minimum and maximum values of α were 0.03391 and 0.03812, respectively, resulting in deviations of about 6%. Actually, most runs were even closer to the true value of 0.036. Similarly, the minimum and maximum values of n were 1.4685 and 1.655, respectively, also representing errors of about 6%. The errors in the estimation of θ_s were of the same order as the superimposed deterministic errors for the initial and final water contents, i.e., 0.02. Deviations in K_s from its true value were higher only for those scenarios when the superimposed errors on the initial and final water contents were of the opposite sign (+/−). Increasing the initial water content and decreasing the final water content caused overestimation of K_s, and vice versa; decreasing the initial water content and increasing the final water content resulted in underestimation of K_s. Still, all final estimates of the soil hydraulic parameters, as presented in Table 4, should be acceptable for most practical situations.

CONCLUSIONS

In this paper, we analyzed five different combinations of multiple tension disc infiltration data for possible numerical estimation of the soil hydraulic properties expressed by analytical functions as given by van Genuchten (1980). We combined the primary multiple tension infiltration curve either with unsaturated hydraulic conductivity values, as obtained using Wooding's analytical solution, or with the water content below the disc infiltrometer associated with the final supply pressure head. The resulting objective functions were analyzed visually by means of response surfaces and numerically by using the Levenberg-Marquart parameter optimization method. The initial conditions were expressed in terms of either the pressure head or the water content. The most promising scenario for practical applications was a combination of the multiple tension cumulative infiltration data with measured final water contents when the initial condition was expressed in terms of the water content. The response surfaces for this scenario showed very well defined global minima in all parameter planes. Also, the inverse solutions identified, for all combinations of optimized parameters and for all initial guesses of the unknown parameters, the true values of the optimized parameters. Superposition of a random er-

ror representing instrumentation and calibration errors on the infiltration data and a deterministic error on the initial and final water contents did yield parameter values that were not unacceptably different, from a practical point of view, from the true values.

REFERENCES

Angulo Jaramillo, R., J.-P. Gaudet, J.-L. Thony, and M. Vauclin. 1996. Measurement of hydraulic properties and mobile water content of a field soil. Soil Sci. Soc. Am. J. 60:710–715.

Ankeny, M. D., T. C. Kaspar, and R. Horton. 1988. Design for an automated tension infiltrometer. Soil Sci. Soc. Am. J. 52:893–896.

Ankeny, M. D., M. Ahmed, T. C. Kaspar, and R. Horton. 1991. Simple field method for determining unsaturated hydraulic conductivity. Soil Sci. Soc. Am. J. 55:467–470.

Bard, Y. 1974. Nonlinear parameter estimation. Academic Press, New York.

Carsel, R. F., and R. S. Parrish. 1988. Developing joint probability distributions of soil water retention characteristics. Water Resour. Res. 24:755–769.

Celia, M. A., E. T. Bouloutas, and R. L. Zarba. 1990. A general mass-conservative numerical solution for the unsaturated flow equation. Water Resour. Res. 26:1483–1496.

Clothier, B. E., M. B. Kirkham, and J. E. McLean. 1992. In situ measurement of the effective transport volume for solute moving through soil. Soil Sci. Soc. Am. J. 56:733–736.

Gardner, W. R. 1958. Some steady-state solutions of the unsaturated moisture flow equation with application to evaporation from a water table. Soil Sci. 85:228–232.

Jarvis N. J., and I. Messing. 1995. Near-saturated hydraulic conductivity in soils of contrasting texture measured by tension infiltrometers. Sci. Soc. Am. J. 59:27–34.

Kool, J. B., J. C. Parker, and M. Th. van Genuchten. 1985. Determining soil hydraulic properties from one-step outflow experiments by parameter estimation: I. Theory and numerical studies. Soil Sci. Soc. Am. J. 49:1348–1354.

Kool, J. B., J. C. Parker, and M. Th. van Genuchten. 1987. Parameter estimation for unsaturated flow and transport models—A review. J. Hydrol. 91:255–293.

Logsdon, S. D., E. L. McCoy, R. R. Allmaras, and D. R. Linden. 1993. Macropore characterization by indirect methods. Soil Sci. 155:316–324.

Logsdon, S. D., and D. B. Jaynes. 1993. Methodology for determining hydraulic conductivity with tension infiltrometers. Soil Sci. Soc. Am. J. 57:1426–1431.

Marquardt, D. W. 1963. An algorithm for least-squares estimation of nonlinear parameters. SIAM J. Appl. Math. 11:431–441.

McLaughlin, D., and L. R. Townley. 1996. A reassessment of the groundwater inverse problem. Water Resour. Res. 32:1131–1161.

Mualem, Y. 1976. A new model for predicting the hydraulic conductivity of unsaturated porous media. Water Resour. Res. 12:513–522.

Perroux, K. M., and I. White. 1988. Design for disc permeameters. Soil Sci. Soc. Am. J. 52:1205–1215.

Press, H. W., B. P. Flannery, S. A. Teukolsky, and W. T. Vetterling. 1989. Numerical recipes; The art of scientific computing. Cambridge University Press, Cambridge.

Quadri, M. B., B. E. Clothier, R. Angulo Jaramillo, M. Vauclin, and S. R. Green. 1994. Axisymetric transport of water and solute underneath a disk permeameter: Experiments and numerical model. Soil Sci. Soc. Am. J. 58:696–703.

Reynolds, W. D., and D. E. Elrick. 1991. Determination of hydraulic conductivity using a tension infiltrometer. Soil Sci. Soc. Am. J. 55:633–639.

Russo, D. 1988. Determining soil hydraulic properties by parameter estimation: On the selection of a model for the hydraulic properties. Water Resour. Res. 24:453–459.

Russo, D., E. Bresler, U. Shani, and J. C. Parker. 1991. Analysis of infiltration events in relation to determining soil hydraulic properties by inverse problem methodology. Water Resour. Res. 27:1361–1373.

Šimůnek, J., and M. Th. van Genuchten. 1996. Estimating unsaturated soil hydraulic properties from tension disc infiltrometer data by numerical inversion. Water Resour. Res. 32:2683–2696.

Šimůnek, J., M. Šejna, and M. Th. van Genuchten. 1996. The HYDRUS-2D software package for simulating water flow and solute transport in two-dimensional variably saturated media. Version 1.0. IGWMC - TPS - 53, International Ground Water Modeling Center, Colorado School of Mines, Golden, CO.

Toorman, A. F., P. J. Wierenga, and R. G. Hills. 1992. Parameter estimation of hydraulic properties from one-step outflow data. Water Resour. Res. 28: 3021–3028.

van Dam, J. C., J. N. M. Stricker, and P. Droogers. 1992. Inverse method for determining soil hydraulic functions from one-step outflow experiment. Soil Sci. Soc. Am. J. 56:1042–1050.

van Dam, J. C., J. N. M. Stricker, and P. Droogers. 1994. Inverse method to determine soil hydraulic functions from multistep outflow experiment. Soil Sci. Soc. Am. J. 58:647–652.

van Genuchten, M. Th. 1980. A closed-form equation for predicting the hydraulic conductivity of unsaturated soils. Soil Sci. Soc. Am. J. 44:892–898.

van Genuchten, M. Th. 1981. Non-equilibrium transport parameters from miscible displacement experiments. Research Report No. 119. U. S. Salinity Laboratory, USDA, ARS, Riverside, CA.

Warrick, A. W. 1992. Model for disc infiltrometers. Water Resour. Res. 28:1319–1327.

Wooding, R. A. 1968. Steady infiltration from large shallow circular pond. Water Resour. Res. 4:1259–1273.